Technical Paper

ISSN 1997-1400 Int. J. Pavement Res. Technol. 8(3):179-184

The Meso Structure and Strain Distribution Analysis of Cement Emulsified Asphalt Concrete

Jun Fu[1+], Xiaoqiang Zhang[1], and Fazhou Wang[1]

Abstract: In this article, the mix design of Cement Emulsified Asphalt Concrete (CEAC) is introduced. A 2-dimensional image of CEAC obtained in meso scale could be distinguished into 3-phase materials that include cement emulsified asphalt mastics, aggregates, and air voids. Then, an FEM model is used to simulate the steady mechanical behaviors of CEAC in which cement emulsified asphalt mastics are defined as dispersions of aggregate fillers within a medium of binder. The virtual indirect tensile test is simulated to study the strain distribution of CEAC and the results show the cement-asphalt binder can be considered as the weak failure phase material. In addition, the influence of mechanical properties of aggregate and cement-asphalt binder are discussed and the results show that the strain distribution of CEAC is sensitive to the elastic modulus of cement-asphalt binder.

DOI: 10.6135/ijprt.org.tw/2015.8(3).179

***Key words**: Cement Emulsified Asphalt Concrete, FEM, Mesostructure, Strain distribution*

Introduction

Cement emulsified asphalt concrete (CEAC) is a composite material formed by Portland cement, emulsified asphalt, graded aggregates, and some admixtures, which can be cool-mixed and cool-spread. Due to presence of cement mortar, the relative proportion of the asphalt in CEAC is reduced, which significantly improves the strength, elastic modulus and durability of CEAC. CEAC is a better choice in comparison with asphalt concrete [1-2]. The effect of adding cement into emulsion-treated mixes (ETM) was studied by Schmidt et al. [3], which explores the use of lime and cement in ETM. Head [4] reported the results of research on cement modified asphalt cold mixes. The use of normal Portland cement in emulsion mixtures was reported by Uemura and Nakamori for several years in Japan [5]. The report pointed out the performance of emulsion mixtures was at an acceptable level, and it was more environmentally friendly. Li et al. [6] conducted experiments to evaluate the mechanical properties of a three-phase cement-asphalt emulsion composite (CAEC). Brown and Needham [7] studied asphalt emulsion mixtures, or cold mix, and proposed that mechanical properties were affected by a number of parameters, including binder grade, void content, curing time, and additives such as cement. Pouliot et al. [8] aimed at understanding the hydration process, the microstructure, and the mechanical properties of mortars prepared with a new mixed binder made of cement slurry and a small quantity of asphalt emulsion (SS-1 and CSS-1).

However, CEAC is a multiphase composite material whose physical properties and performance are intimately related to its mesostructures. A general finite element method to simulate particulate and heterogeneous materials has been used as an equivalent lattice network system to represent the interparticle load transfer behavior. This type of asphalt microstructural modeling has been used previously by Bazant et al. [9], Mora [10], Sadd and Gao [11], and Budhu et al. [12]; Bahia et al. [13] have also used finite elements to model the aggregate-mastic response of asphalt materials. Mustoe and Griffiths [14] developed an FEM, which was similar to a particular discrete element method (DEM).

In summary, previous studies of CEAC usually included mix design and the development of the mechanical properties of CEAC. Therefore, limited research has been available on the mesostructure of CEAC and the strain distribution until now. This paper focuses on the generation of the mesostructure of CEAC and FEM model. In this study, CEAC is considered as multi-phase composite material that includes aggregates, cement-emulsion paste, and air voids. Then, the influence of material properties of the component on CEAC's strain distribution is analyzed by a virtual indirect tensile simulation. It is believed that this study will add new contributions to the field of CEAC and its application.

Material and Specimen Preparation

The material used in this study is emulsified asphalt, Portland cement, fly ash, aggregates, water, and additives. The CEAC mix design is shown in Table 1. Aggregate type on determination of the emulsion type is anionic. Aggregates, cement, and fly ash are prepared by first mixing for three minutes. Then, emulsified asphalt and water reducer are added to the dry mixture and mixed for five minutes. Emulsified asphalt is comprised organic cementitious materials, and cement is comprised of inorganic cementitious materials; both of them form a solid, flexible and rigid integral composite material.

Meso Structural Finite-Element Analysis of CEAC

Meso-structure of CEAC

From the image of the cross section (Fig. 1), CEAC can only be distinguished clearly with aggregates, asphalt-cement binder and a

[1] Wuhan University of technology, Wuhan 430063, China.

[+] Corresponding Author: mail fjgrant@whut.edu.cn

Note: Submitted October 25, 2014; Revised January 29, 2015; Accepted February 13, 2015.

Table 1. CEAC Mix Design.

Material	Cement	Aggregates	Emulsified Asphalt	Water reducer	Reference	
Specifications	P.O42.5	AC-20C	Anionic	Poly Carboxylic Acid	Asphalt Aggregates Ratio	Cement content
Content of Mixture（kg/m³）	150	2000	140	1.5	7%	5%

few air voids. The mesostructure image of CEAC (Fig. 2(a)) was created by a self-developed image processing application [15]. So in meso scale, CEAC can be described as a multi-phase material containing aggregate, asphalt-cement binder (including mastic and fine particles), and air voids (Fig. 2(b)).

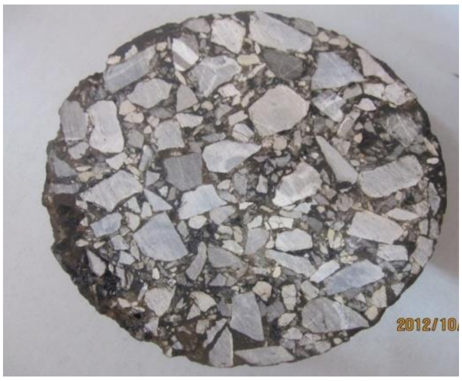

Fig. 1. Cross section of CEAC.

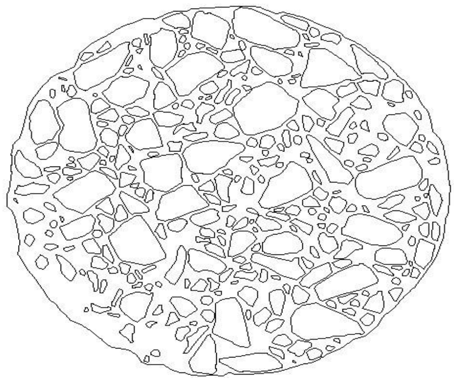

(a)

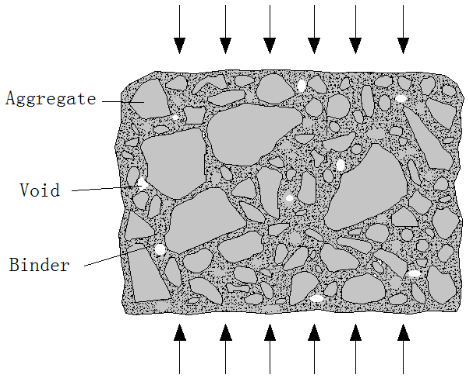

(b)

Fig. 2. (a) Meso Structural Image of CEAC; (b) Meso Structure of CEAC.

Meso-structure FEM Model of CEAC

Finite element method (FEM) is similar to a particular discrete element method. In meso-scale, FEM is more convenient and easier than DEM. According to the results of the test, aggregates and cement-asphalt are considered as linear elastic material at a temperature of 25°C, and the analysis is linear in this study. The elastic properties of aggregates and asphalt-cement binder are shown in Table 2. A 2D strain finite-element model is developed by ANSYS. The element Plane182 is used for 2-D modeling of solid structures. The element can be used as either a plane element (plane stress, plane strain, or generalized plane strain) or an axisymmetric element. It is defined by four nodes having two degrees of freedom at each node: translations in the nodal x and y directions, which can be defined by four nodes having two degrees of freedom at each node, are selected for FEM analysis. A total number of 39,190 elements are used in this particular FE model.

Consequently, finite-element analysis of the CEAC meso-structure is performed to capture the strain distribution at smaller localized areas. Fig. 3 shows the meso-structure FE model which created from the 2D image of a cross section of CEAC. The diameter of the model is 101.6 mm. As a multiphase composite, CEAC includes very irregular aggregates, complex distributed cement-asphalt binder, and air void. So CEAC is divided into three different subdomains, but the air voids in this example are very small. Elements share the nodes in neighboring boundary. The elastic modulus of asphalt-cement binder at 25°C is selected according to test results. An FEM model of CEAC has been developed for virtual indirect tension test (IDT) simulation that is commonly used to determine the tensile or splitting strength of bituminous materials, in which model boundary conditions constrain both horizontal and vertical displacements of the bottom pair of aggregates, while the top particle pair accept the applied vertical displacement (Fig. 4).

Results and Discussion

Strain Distribution and Failure Criterion

To avoid variations in strain magnitudes due to boundary effects, the area analyzed is the major part of the image, and it is symmetrical around the center point of the specimen surface. An example of the strain distributions obtained from the vertical loading -0.2 mm simulation specimens is presented in Figs. 5 to 10.

Table 2. Properties of CEAC Finite-Element Model.

Material	Modulus of Elasticity (MPa)	Poisson’s Ratio	Ultimate Tensile Strength (με)
Aggregate	$55.5\text{x}10^5$	0.16	97
Asphalt-cement Binder	$1\ \text{x}10^3$	0.24	1080

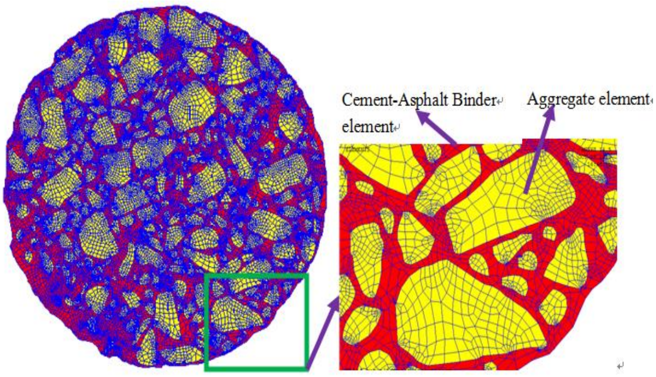

Fig. 3. FE Meshes of CEAC.

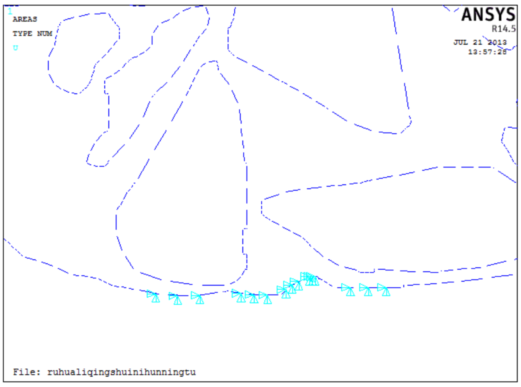

Fig. 4. Loading Condition of IDT Simulation.

The horizontal strain component εx of aggregates in the vertical direction, especially near the center of the circle, is mostly tensile along the diameter from Fig. 5. Meanwhile, the strain away from the center of circle is mostly compressive. In the vertical direction, only part of the elements near the center of the circle is tensile strain. The number of tensile elements is smaller than the compressive elements. Statistics are based on ANSYS post-processing, in which about 30.70% aggregates elements are compressive and tensile elements are 69.30%. As for the vertical strain components ε_y, most of the aggregate elements are compressive, as shown in Fig. 8. For cement-asphalt binder, some elements in ε_x are tensile, which is not far away from the y-direction symmetry axis. However, most of the cement-asphalt binder elements in ε_y are compressive with few tensile elements, according to Fig. 8. Figs. 5 and 7 show the maximum cement-asphalt binder strain value ε_x is 2624 με, as high as 17.5 times of the aggregate strain, which is 150 $\mu\varepsilon$. About 69.30% of elements in ε_x are tensile and 30.70% are compressive, as shown in Figs. 9 and 10.

According to test results, cement-asphalt binder and aggregates are both considered as linear elastic brittle material at temperature 25°C, so maximum principal strain criterion can be chosen for yield criterion.

$$\left\{\begin{matrix}\varepsilon_1 \\ \varepsilon_3\end{matrix}\right. = \frac{\varepsilon_x+\varepsilon_y}{2} \pm \sqrt{(\frac{\varepsilon_x-\varepsilon_y}{2})^2+(\frac{\gamma_{xy}}{2})^2} \tag{1}$$

$$\varepsilon_{max} = \varepsilon_1 = \frac{1}{E}[\sigma_1 - \mu(\sigma_2+\sigma_3)] \tag{2}$$

When $\varepsilon_{max} \geq \varepsilon_u$, the material fractures.

The stress state of CEAC is shown in Figs. 11 and 12. From Figs.

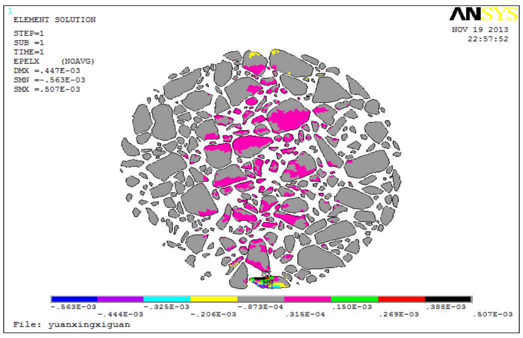

Fig. 5. Aggregates Strain ε_x .

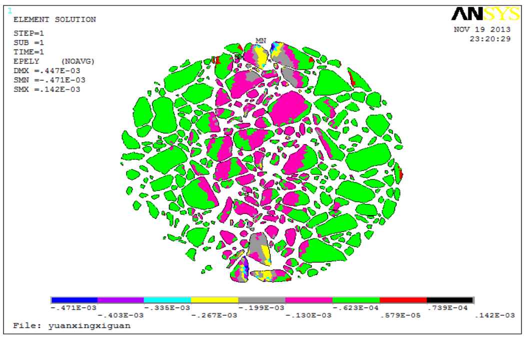

Fig. 6. Aggregates Strain ε_y .

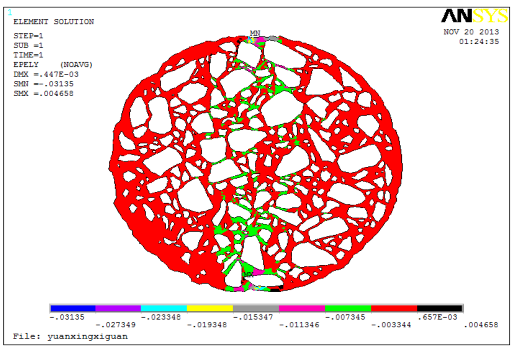

Fig. 7. Cement-Asphalt Binder Strain ε_x .

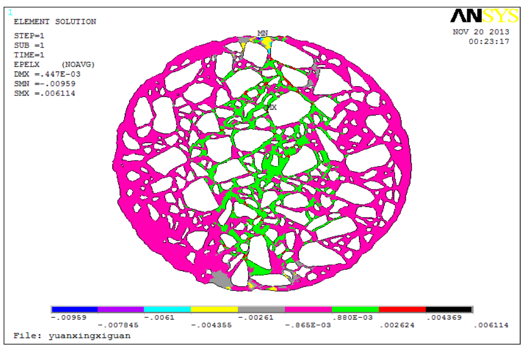

Fig. 8. Cement-Asphalt binder strain ε_y .

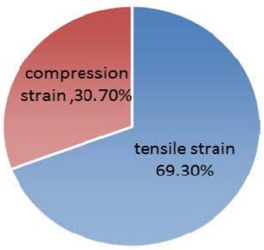

Fig. 9. Aggregates Strain Ratio.

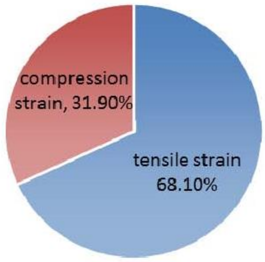

Fig. 10. Cement-Asphalt Binder Strain Ratio.

13 to 14, the stress distribution is in the specimen center symmetry. ε_1 is assumed as the largest principal strain that failure has occurred if ε_1 is greater than ultimate tensile strength. Figs. 13 and 15 show that there are only 1.14% of aggregate elements, in which ε_1 is over than ultimate tensile strength. On the contrary, there are about 24.97% of cement-asphalt binder elements for which ε_1 values are larger than ultimate tensile strength 1080 με, as shown in Figs. 13 and 16. According to the maximum strain criterion, the strain causes failure. So the weak failure phase material is cement-asphalt binder. Indirect tensile experiment results also prove that the CEAC cracks appeared in the vicinity of cement-asphalt binder (Fig. 17).

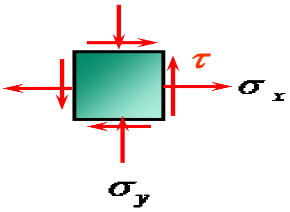

Fig. 11. Stress States.

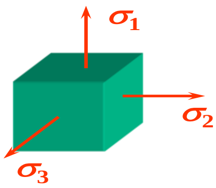

Fig. 12. Principle Stress States.

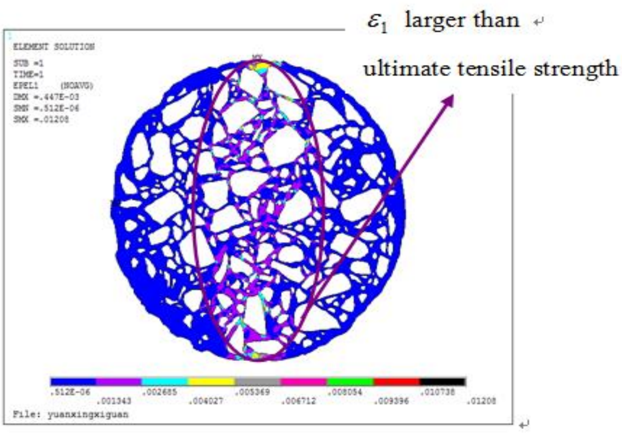

Fig. 13. Cement-Asphalt Binder Strain ε_1.

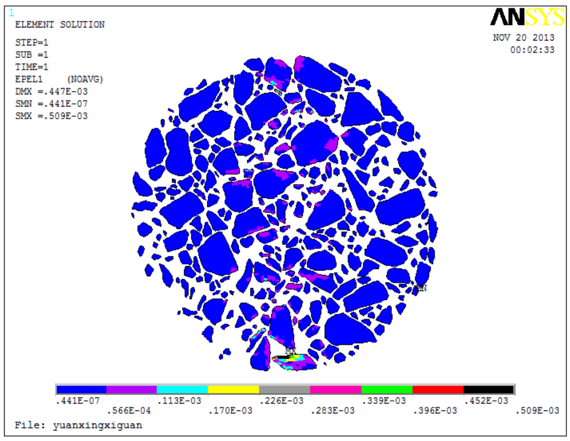

Fig. 14. Aggregates Strain ε_1.

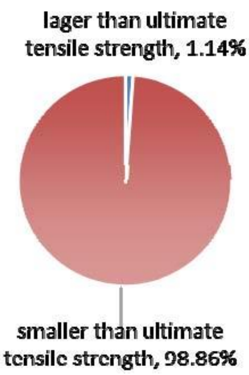

Fig. 15. Aggregates Strain ε_1.

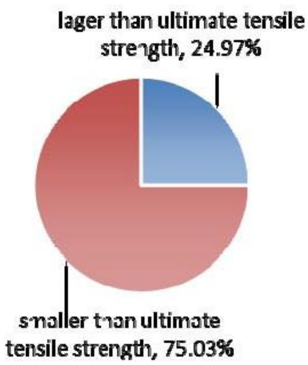

Fig. 16. Cement-Asphalt Binder Strain ε_1.

Fig. 17. CEAC Indirect Tensile Test Fracture.

Cement-asphalt Binder Sensitivity Analysis.

In CEAC, aggregate and cement-asphalt binder are considered as two phase components, but the properties of cement-asphalt binder could be changed to analyze the influence on the CEAC mechanical characters. In Fig. 18, the x-axis represents the elastic modulus of cement-asphalt binder and the y-axis represents ε_1 value of the element No 36478 by FEM analysis. Fig. 19 is the same as Fig. 21, except that the element No 7839 is aggregate. Fig. 18 shows the strain value of cement-asphalt binder decreases as the elastic modulus grows. When elastic modulus of cement-asphalt binder changes from 600 MPa to 1200 MPa, the corresponding strain value decreases from 1627 to 1569 $\mu\varepsilon$, which is only 3.5%. The influence of elastic modulus on aggregate is more sensitive than its influence on cement-asphalt binder. Fig. 19 shows that the strain of aggregate grows when elastic modulus of cement-asphalt binder increases. When elastic modulus increases from 600 to 1200 MPa, the strain value of aggregate raises from 15.3 to 27.3, i.e. up to 78.4%, but the strain value is far less than ultimate tensile strength, which is 97 με. As for Poisson's ratio of cement-asphalt binder, the strain of aggregate and cement-asphalt binder are both urging positive linear growth, as seen in Figs. 20 and 21. When Poisson's ratio of binder changes from 0.20 to 0.27, the value of element No 36478 increases by only 6.3%.The effect of Poisson's ratio of aggregates is also small and can be ignored.

Conclusion

This paper introduces the mix design and specimen preparation of CEAC. Then, a two-dimensional meso structural image of CEAC is achieved, which is numerically created from surface photographic data of an actual CEAC sample. This is accomplished through a self-developed image process application. Then a two-dimensional mesomechanical FEM model is developed to analyze the strain distribution of CEAC by virtual indirect tension test simulation. The design samples are numerically subjected to the loading and constraints of typical IDT tests, in which horizontal strain is tensile and vertical strain is compressive. The mesomechanics analysis indicates that the maximum cement-asphalt binder strain value is about 17.5 times the aggregates strain. Moreover, the findings of this study show that there are some cement-asphalt binder elements which have larger than ultimate tensile strength while having aggregates strain condition within the safe range. The crack of CEAC appears near the cement-asphalt binder and it is shown by

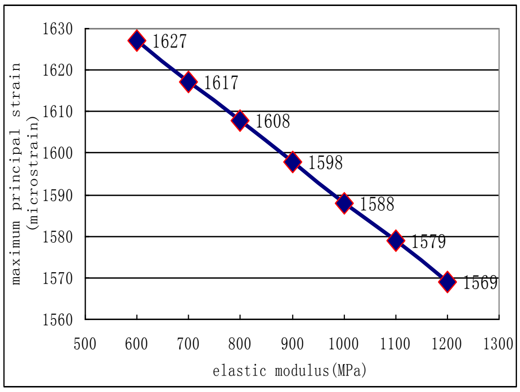

Fig. 18. Influence of Binder's Modulus.

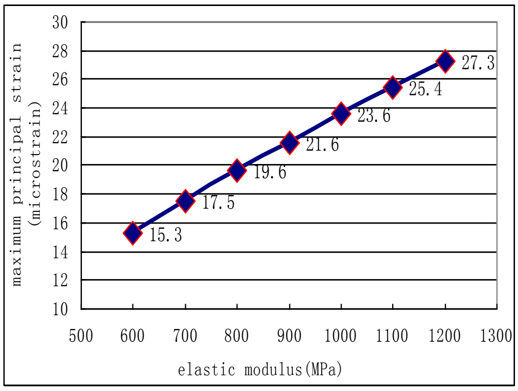

Fig. 19. Influence of Aggregate's Modulus.

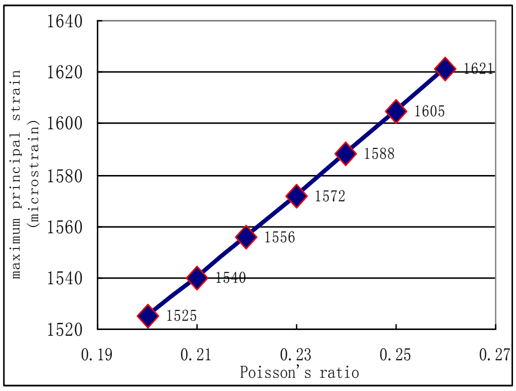

Fig. 20. Influence of Binder's Poisson's Ratio.

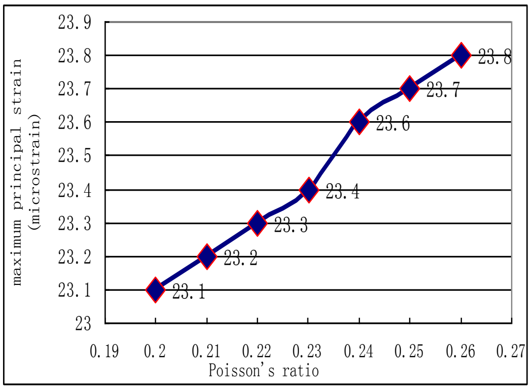

Fig. 21. Influence of Aggregate's Poisson's Ratio.

test results. The results of this study also indicate that:

1) In meso scale, CEAC could be distinguished into 3-phase materials that include cement-asphalt binder, aggregates, and voids.
2) The weak failure phase material of CEAC is cement-asphalt binder.
3) The elastic modulus of cement-asphalt binder could exert the most influence over the strain distribution. In addition, the influence of aggregates' elastic modulus on strain distribution is smaller and can even be ignored.
4) As for Poisson's ratio, both cement-asphalt binder and aggregates had low impact on the strain distribution of CEAC.

However, the current two-dimensional meso structural model is limited to the analysis of the strain distribution of CEAC only. The analysis in this study is only linear. Future work will pursue in more detail these damage comparisons between the mesomechanical model and data on real CEAC. Simulations will also be conducted to predict the mechanical properties of CEAC in meso scale. The influence of moisture in CEAC will be considered in the future as well.

Acknowledgements

The authors would like to acknowledge support by the National Natural Science Foundation of China (Nos.51072149) along with additional support by the Chinese Department of Transportation Planning Project of Science and Technology (Nos.2015319811320) and Hubei Highway Planning Project of Science and Technology (Nos.2014).

References

1. Yu, C., Fu, J. (2011). Research of Semi-flexible Cement Emulsified Asphalt Concrete Surface Layer Material, *Construction Material World*, 32(1), pp. 26-29 (in Chinese).
2. Hu, L.-Q., Sha, A-M. Road Performance of Vibration-compaction Emulsified-asphalt Cement Concrete, *Journal of Chang'an University: Natural Science Edition*, 200; 27(02), pp. 12-15 (in Chinese).
3. Schmidt, R.J., Santucci, L.E., and Coyne, L.D. (1973). Performance Characteristics of Cement Modified Asphalt Emulsion Mixes, *Association of Asphalt Paving Technologists Conference Proceedings,* 42, pp. 300–319.
4. Head, R.W. (1974). An Informal Report of Cold Mix Research Using Emulsified Asphalt as a Binder, *Association of Asphalt Paving Technologists Conference Proceedings,* 43, pp. 110–131.
5. Uemura, T. and Nakamori, Y. (1993). Stabilization Process of Cement Asphalt Emulsion in Japan. First World Congress on Emulsions, 4-13-16/01-06.
6. Li, G., Zhao, Y., Pang, S.S., and Huang, W. (1998). Experimental Study of Cement-Asphalt Emulsion Composite. *Cement Concrete Research,* 28(5), pp. 635–641.
7. Brown, S.F. and Needham, D. (2000). A Study of Cement Modified Bitumen Emulsion Mixtures, *Association of Asphalt Paving Technologists Conference Proceedings*, 2, pp. 92-121
8. Pouliot, N., Marchland, J., and Pigeon, M. (2003). Hydration Mechanisms, Microstructure, and Mechanical Properties of Mortars Prepared with Mixed Binder Cement Slurry-Asphalt Emulsion, *Journal of Materials in Civil Engineering*, 15(1), pp. 54–59.
9. Bazant, Z.P., Tabbara, M.R., Kazemi, Y., and Pijaudier-Cabot, G. (1990). Random Particle Simulation of Damage and Fracture in Particulate or Fiber-Reinforced Composites, *Damage Mechanics in Engineering Materials, Transportation ASME*, 109, pp. 41-55.
10. Mora, P. (1992). A Lattice Solid Model for Rock Rheology and Tectonics, The Seismic Simulation Project, Tech. Institute de Physique du Globe, Paris, 4, pp. 3-28.
11. Sadd, M.H. and Gao, J.Y. (1998). Contact Micromechanics Modeling of the Acoustic Behavior of Cemented Particulate Marine Sediments, *Proceedings of the 12th ASCE Engineering Mechanics Conference,* La Jolla, CA, USA.
12. Budhu, M., Ramakrishnan S., and Frantziskonis, G. (1997). Modeling of Granular Materials: A Numerical Model Using Lattices, Mechanics of Deformation and Flow of Particulate Materials, Ed. C.S. Chang, A. Misra, R.Y. Liang and M. Babic, *Proceedings of McNu Conference, Transportation ASCE,* Northwestern University, pp. 77-90.
13. Bahia, H., Zhai, H., Bonnetti, K., and Kose, S. (1999). Nonlinear Viscoelastic and Fatigue Properties of Asphalt Binders, *Journal of the Association of Asphalt Paving Technology,* 68, pp. 1–34.
14. Mustoe, G.G.W. and Griffiths, D.V. (1998). An Equivalent Continuum Model using the Discrete Element Method (DEM), ASCE Specialty Conference - Engineering Mechanics, San Diego, USA, pp. 989-992.
15. Fu, J., Shi, Z., Dai, D., and Huang J. (2013). Microstructure Analysis for Emulsified Asphalt Cement Concrete, *Advanced Materials Research,* 818, pp. 20-23.